Improved description of soft layered materials with van der Waals density functional theory

2012 J. Phys.: Condens. Matter 24 424216

(http://iopscience.iop.org/0953-8984/24/42/424216)

IOP PUBLISHING JOURNAL OF PHYSICS: CONDENSED MATTER

J. Phys.: Condens. Matter **24** (2012) 424216 (8pp) doi:10.1088/0953-8984/24/42/424216

Improved description of soft layered materials with van der Waals density functional theory

Gabriella Graziano[1,2], Jiří Klimeš[1], Felix Fernandez-Alonso[2,3] and Angelos Michaelides[1]

[1] Thomas Young Centre, London Centre for Nanotechnology and Department of Chemistry, University College London, London WC1E 6BT, UK
[2] ISIS Facility, Rutherford Appleton Laboratory, Chilton, Didcot, Oxfordshire OX11 0QX, UK
[3] Department of Physics and Astronomy, University College London, London WC1E 6BT, UK

E-mail: angelos.michelides@ucl.ac.uk

Received 26 March 2012, in final form 6 July 2012
Published 3 October 2012
Online at stacks.iop.org/JPhysCM/24/424216

Abstract
The accurate description of van der Waals forces within density functional theory is currently one of the most active areas of research in computational physics and chemistry. Here we report results on the structural and energetic properties of graphite and hexagonal boron nitride, two layered materials where interlayer binding is dominated by van der Waals forces. Results from several density functionals are reported, including the optimized Becke88 van der Waals (optB88-vdW) and the optimized PBE van der Waals (optPBE-vdW) (Klimeš *et al* 2010 *J. Phys.: Condens. Matter* **22** 022201) functionals. Where comparison to experiment and higher-level theory is possible, the results obtained from the two new van der Waals density functionals are in good agreement. An analysis of the physical nature of the interlayer binding in both graphite and hexagonal boron nitride is also reported.

(Some figures may appear in colour only in the online journal)

1. Introduction

Recent years have seen a surge of interest in understanding the role of van der Waals (dispersion) forces in chemistry, physics, and materials science. It has long been recognized that dispersion forces are fundamental for the stability of DNA and protein structures [1, 2], but they are also present in solids [3–5] and it has been found that an accurate description of dispersion forces is needed in processes like adsorption [6–8] and molecular self-assembly [9]. The fervent research into van der Waals dispersion forces is also driven by a desire to overcome the challenge they represent for theoretical approaches based on density functional theory (DFT) [10, 11]. Indeed, several schemes within DFT have now been proposed that account for dispersion in one way or another [12–20]. Although the accuracy of these methods has been established in many circumstances—particularly for purely van der Waals bonded systems—how they perform in the description of systems where both strong (covalent and ionic) and weak (van der Waals) bonding is involved is less clear.

Of the various schemes available for accounting for van der Waals forces within DFT, we concentrate here mainly on the class of functionals based on the non-local van der Waals functional of Dion *et al* [16]. The original Dion *et al* exchange–correlation functional, generally known as vdW-DF, is defined as:

$$E_{\mathrm{xc}}[n] = E_{\mathrm{revPBE}(x)}[n] + E_{\mathrm{LDA(c)}}[n] + E_{\mathrm{nl(c)}}[n] \qquad (1)$$

where $E_{\mathrm{revPBE}(x)}[n]$ is the exchange energy obtained with the revPBE functional [21]. $E_{\mathrm{LDA(c)}}[n]$ is a local-density approximation (LDA) correlation and $E_{\mathrm{nl(c)}}[n]$ is a non-local correlation term which captures (approximately) van der Waals interactions. In 2010, Lee *et al* proposed a new version of vdW-DF, known generally as vdW-DF2 [22]. This version uses a modified Perdew Wang 86 (PW86) [23, 24] exchange functional and a modified gradient dependence of the non-local correlation energy. To improve upon the

original vdW-DF, Klimeš *et al* developed the optimized Becke88 [25] van der Waals (optB88-vdW) and the optimized Perdew–Burke–Ernzerhof (PBE) [26] van der Waals (optPBE-vdW) [27] functionals, which differ from the Dion *et al* functional only in the exchange term. Specifically, in the optB88-vdW a reparametrized version of the Becke88 exchange functional is used in (1) and in the optPBE-vdW functional a modified PBE functional is used in (1). These alternative exchange functionals were obtained by fitting to the S22 dataset [27] (a benchmark set of weakly bonded dimers for which structures and energies have been accurately determined) and in so-doing much improved interaction energies over the original vdW-DF of Dion *et al* were obtained. The optB88-vdW and optPBE-vdW functionals have by now been shown to perform well on a wide variety of gas phase clusters, solids and adsorption problems [3, 6, 27–31]. However, considerably more work is required to establish how widely applicable and generally useful these functionals are, particularly for condensed matter systems.

Here we report the results of DFT calculations on graphite and hexagonal boron nitride (h-BN) to evaluate the performance of several exchange–correlation functionals and to understand and compare the nature of the interlayer binding in the two materials. Graphite and h-BN are interesting materials to compare because, despite their different chemical composition, their interlayer spacings are essentially the same, but why this is so is not completely understood. Furthermore, their anisotropic nature, with strong covalent intralayer bonds and much weaker interlayer bonds, dominated by van der Waals interactions, makes them challenging and intriguing materials to explore with theory. This anisotropy is, of course, also key to many of the technological applications (e.g. lubrication [32], batteries [33], or gas storage [33–37]) of these soft layered materials.

Graphite and h-BN have been widely examined before with theoretical methods and are increasingly being considered as model benchmark systems against which new methods are tested [19, 38–42]. By now, it is largely recognized that the PBE functional within the generalized-gradient approximation (GGA) fails to reproduce any significant interlayer bonding and that LDA gives bulk properties that are closer to experiment [38–41, 43]. However, the superior performance of LDA in this regard is known to be fortuitous, as LDA relies on a local description of exchange and correlation and does not account for non-local interactions. Several of the functionals developed to give a more accurate treatment of van der Waals forces, (e.g. the approaches based on C_6 corrections to DFT [18, 44] and vdW-DF and vdW-DF2) have already been applied to graphite and h-BN and do, on the whole, offer improved performance [15, 44–48]. Also, highly expensive approaches based on the random phase approximation (RPA) [49] and quantum Monte Carlo (QMC) have been applied, yielding interlayer binding energies in good agreement with experiment [19, 42, 50].

In the following we present results obtained with the optB88-vdW and optPBE-vdW functionals as well as several others (LDA, PBE, PBE with the empirical dispersion correction of Grimme [51] and vdW-DF2) for the description of the intralayer and interlayer binding of graphite and h-BN. We also bring together results from a variety of other functionals and theoretical methods so that a clear picture of the current state of the field can be obtained. Moreover, a brief analysis of the nature of the interlayer bonding in both materials is presented. In section 2 details of the computational setup are provided. Following this, in section 3 the main results are reported and in section 4 we close with a discussion and some conclusions.

2. Methods

The DFT calculations have been performed with the periodic plane-wave basis set code VASP 5.2 [52–54] and six different exchange–correlation functionals, namely, LDA, PBE, PBE with an empirical dispersion correction of Grimme (DFT-D2), vdW-DF2, optB88-vdW, and optPBE-vdW. The calculations with the vdW correlation functional have been carried out self-consistently using an implementation [3] of the vdW-DF method [16] in VASP with the scheme of Román-Pérez and Soler [55].

Projector-augmented-wave [56] (PAW) potentials have been used, with LDA-based PAW potentials for the LDA calculations and PBE potentials for the PBE and all the various vdW-DF based calculations[4]. All results reported have been obtained with hard potentials using a very high (900 eV) plane-wave cut-off [5].

Two-atom unit cells of height 7 Å were used to calculate bond lengths and bond strengths within the isolated two-dimensional graphite or h-BN layers. The unit cells used to calculate the interlayer distances in bulk graphite and h-BN contained two AB-stacked layers. Periodic boundary conditions have been applied and thus the two layers in the unit cell are representative of the entire periodic crystal. The interlayer distance was changed by varying the cell dimensions along the z-axis over the range 5–14 Å. The h-BN calculations were also performed using an AA′ stacking sequence where boron and nitrogen were placed on top of each other. We used a Monkhorst–Pack k-point grid of $24 \times 24 \times 2$ per (1×1) unit cell for graphite and $8 \times 8 \times 2$ per (1×1) unit cell for h-BN, which ensured that bond lengths

[4] For the calculations with the optB88-vdW functional we used both LDA and PBE potentials and found that the bond lengths and energies obtained differed by <0.001 Å and <1 meV, respectively. This suggests that for the systems considered here, it is not necessary to generate new PAW potentials for the various vdW-DFs. The vdW-DFs treat the exchange–correlation energy as defined by (1) where the first two terms, the exchange and LDA correlation energies, are calculated considering all the electrons within the PAW method as in the PBE calculations. While the last term, the non-local correlation energy, is calculated within a pseudopotential approximation, it has been shown to represent a valid approximation on a wide range of systems [3].

[5] In keeping with our desire to provide well-converged results, we note that these settings are somewhat extreme. Tests with standard PAW potentials and a 600 eV cut-off yielded very similar results. Specifically, differences in calculated distances were $\lesssim \pm 0.002$ Å and differences in calculated energies were $\lesssim \pm 0.02$ eV for the atomization energy and ± 2 meV for the interlayer binding when normal and hard PAWs were compared.

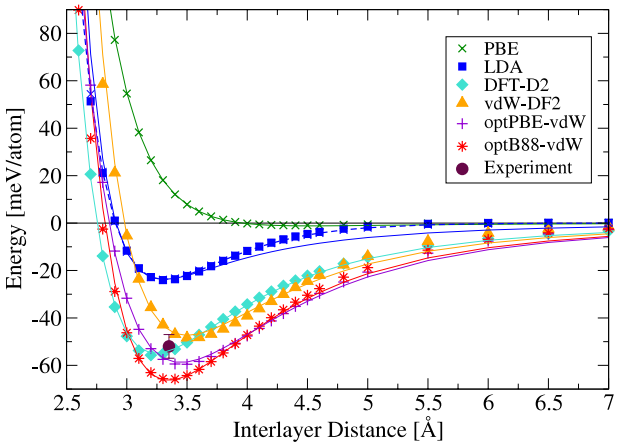

Figure 1. Binding energies as a function of interlayer distance in graphite. The discrete computational data (symbols) have been fitted to the potential: $E = a_0 \exp(-b_0 x) + e_0/x^4$.[6] As the LDA considers atomic attraction to be dependent on electron-density overlap, the LDA fit (dark blue line) shows that the $1/x^4$ asymptotic behavior is not recovered. Better agreement is obtained when the second term is replaced by $a_1 \exp(-b_1 x)$ (dashed dark blue line). Experimental values are taken from [59] for the interlayer distance and from [57] for the energy.

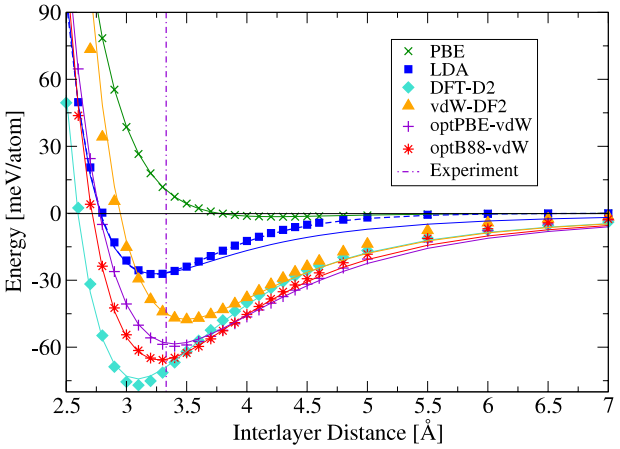

Figure 2. Binding energies as a function of interlayer distance in hexagonal boron nitride with the AA′ stacking. The discrete computational data (symbols) have been fitted to the potential: $E = a_0 \exp(-b_0 x) + e_0/x^4$ (see footnote 6). As the LDA considers atomic attraction to be dependent on electron-density overlap, the LDA fit (dark blue line) shows that the $1/x^4$ asymptotic behavior is not recovered. Better agreement is obtained when the second term is replaced by $a_1 \exp(-b_1 x)$ (dashed dark blue line). The experimental value of the interlayer distance (indicated by the vertical line) is taken from [67].

and energies were converged to within 0.01 Å and 1 meV, respectively.

Atomization energies (E_{atom}) are defined as

$$E_{\text{atom}} = \frac{E_{\text{lay}} - E_{\text{isolated}}}{2}, \tag{2}$$

where E_{lay} is the total energy of a single layer of graphite or h-BN in the two-atom unit cell, and E_{isolated} is the total energy of the isolated atoms in the gas phase. The energies of the isolated atoms were obtained from spin-polarized calculations in a $12 \times 14 \times 16$ Å^3 box with Γ-point sampling of k space.

The interlayer binding energies of the bulk materials have been calculated by subtracting twice the energy of an isolated monolayer of graphite or h-BN (E_{lay}) from the energy of a graphite or h-BN bulk slab (E_{bulk}) and dividing this value by the total number of atoms (N) in the unit cell:

$$E_{\text{inter}} = \frac{E_{\text{bulk}} - 2E_{\text{lay}}}{N}. \tag{3}$$

As a result of the periodic boundary conditions, the calculated interlayer binding energy represents the energy difference per layer between the bulk and the isolated layers. Hanke [48] and Björkman *et al* [5] have shown, based on additivity arguments, that the interlayer binding energy is equivalent to the exfoliation energy. The latter is the energy required to take off the top layer from the material surface as measured by Zacharia *et al* for graphite [57].

The effects of zero point energy (ZPE) on the interlayer binding energy and interlayer spacing have been estimated by considering a first-order harmonic correction to the interlayer potential energy. In this case, the ZPE is simply given by half the characteristic vibrational frequency. This ZPE contribution is added to the total dissociation energy which assumes static (i.e., infinitely heavy) atomic nuclei. The displacement due to ZPE motions has been estimated by calculating the average distance of the ZPE level on the binding energy curves reported in figures 1 and 2. Overall, as shown in tables 2 and 4, ZPE effects are small in these systems ($\lesssim$5 meV and $\lesssim$0.05 Å on interlayer binding energies and distances, respectively) and insensitive to the functional used.

The elastic constant in the c-direction (C_{33}) has been calculated for both materials from the second derivative of the interlayer binding curve with respect to interlayer spacing c using:

$$C_{33} = \frac{2c_0}{\sqrt{3}a_0^2} \frac{\partial^2 E}{\partial c^2}. \tag{4}$$

Here, c_0 is the interlayer distance corresponding to the minimum, $\sqrt{3}a_0^2$ is the area of the unit cell, and E is the total energy.

3. Results

Table 1 reports results for the C–C bond length and atomization energies for a single layer of graphite (graphene) obtained with the various functionals used in this study. From table 1 it can been seen that all functionals considered give similar values for C–C bond lengths, 1.41–1.42 Å, in very good agreement with experiment. Turning to the atomization energies, LDA substantially overestimates the atomization energy by almost 20%, in line with previous calculations [38]. The other functionals offer much better agreement with

[6] Buckingham potential: $E = a\exp(-bx) + e/x^6$, where a, b and e are constants and x is the interatomic distance. The first term describes the repulsion and the second one describes the attraction between two particles. Due to the integration over a surface, this term turns out to depend on x^{-4}.

Table 1. C–C bond lengths and atomization energies for a single layer of graphite (graphene) obtained in this work along with a comparison with other theoretical results and experiment. The experimental value for the atomization energy with ZPE (0.16 eV) [58] removed is reported in square brackets.

Method	Bond length (Å)	E_{atom} (eV/atom)
This work		
optB88-vdW	1.422	−7.55
optPBE-vdW	1.426	−7.65
vdW-DF2	1.428	−6.95
DFT-D2	1.424	−7.99
LDA	1.412	−8.96
PBE	1.424	−7.93
Other work		
LDA	1.413 [38]	−8.89 [38]
vdW-DF for layered materials	1.426 [15]	—
RPA	—	∼ −7.0 [19]
Experiment	1.421 [59]	∼ −7.37 [38] [−7.53]

Table 2. Interlayer distances, interlayer binding energies, and elastic constant, C_{33}, for graphite obtained in this work along with a comparison with other calculations and experiment. Values in square brackets have been corrected for ZPE effects as described in the text.

Method	Interlayer distance (Å)	E_{inter} (meV/atom)	C_{33}(GPa)
This work			
optB88-vdW	3.36 [3.39]	−65 [−61]	38
optPBE-vdW	3.46 [3.48]	−60 [−56]	32
vdW-DF2	3.54 [3.58]	−48 [−44]	33
DFT-D2	3.21 [3.27]	−55 [−52]	36
LDA	3.31 [3.36]	−24 [−21]	31
PBE	∼4	∼ −2	—
Other work			
LDA	3.29 [38]	—	—
	3.30 [42]	−24 [42]	—
	3.33 [50]	−24 [50]	—
	—	—	29 [60]
vdW-DF for layered materials	3.76 [15]	−24 [15]	—
	3.76 [61]	−22 [61]	
vdW-DF	3.59 [45]	−53 [45]	—
vdW-DF2	3.47 [46]	−53 [46]	—
	3.48 [62]	−53 [62]	
TS-PBE	3.33 [48]	−85 [48]	—
DFT-D3	—	−49 [44]	—
RPA	3.34 [50]	−48 [50]	—
QMC	3.35 [42]	−56 [42]	—
Experiment	3.33 [59]	−52± 5 [57]	36±1 [60]

experiment, coming within about 5% of the experimental value. The optB88-vdW functional performs particularly well in this regard, predicting an atomization energy essentially the same as the ZPE-corrected experimental value of −7.5 eV/atom.

The experimental interlayer spacing of graphite is well established at 3.33 Å [59]. The interlayer binding energy (exfoliation energy) is less well established and has been estimated to be −52 ± 5 meV/atom from extrapolations based on temperature-programmed desorption experiments of polycyclic aromatic hydrocarbons from the basal plane of graphite [57]. Accurate explicitly correlated electronic structure techniques (QMC [42] and RPA [19]) agree well with the experimental interlayer spacing (table 2) and predict interlayer binding energies which straddle the experimental value (−48 to −56 meV/atom), suggesting that the estimated experimental value is reasonable. The results for graphite interlayer distances and interlayer binding energies obtained with the various functionals considered in this study are reported in table 2 and figure 1. These show, as seen in previous work, that PBE gives essentially no binding between the layers, except for a very shallow minimum (∼2 meV/atom) at around 4 Å. Fortuitously, LDA predicts a binding energy minimum in good agreement with the experiment (3.31 Å). However, the binding energy is underestimated (−20 meV/atom) and the energy incorrectly decays exponentially as the layer separation is increased (figure 1), since LDA does not take explicit account of long-range interactions. Turning now to the functionals which account for dispersion, clear improvements are observed. DFT-D2 reproduces very well the interlayer binding energy, predicting a value of −55 meV/atom, but slightly underestimates the interlayer distances by ∼3% (3.21 Å). vdW-DF2 also predicts the interlayer binding energy minimum in good agreement with experiment (−48 meV/atom), but overestimates the

Table 3. B–N bond lengths and atomization energies for a single layer of hexagonal boron nitride obtained in this work along with a comparison with other theoretical results and experiment.

Method	Bond length (Å)	E_{atom} (eV/atom)
This work		
optB88-vdW	1.449	−7.04
optPBE-vdW	1.452	−6.91
vdW-DF2	1.455	−6.66
DFT-D2	1.450	−7.08
LDA	1.437	−8.03
PBE	1.450	−7.02
Other work		
LDA	1.420 [63]	−8.09 [63]
	1.435 [64]	—
vdW-DF for layered materials	1.449 [15]	—
Experiment	1.446 [65]	—

Table 4. Interlayer distances and interlayer binding energies for hexagonal boron nitride obtained in this work along with a comparison with other calculations and experiment. Values in square brackets have been corrected for ZPE effects as described in the text.

Method	Interlayer distance (Å)	E_{inter} (meV/atom)	C_{33} (GPa)
This work			
optB88-vdW	(AB) 3.30 [3.31]	−65 [−60]	—
	(AA′) 3.30 [3.32]	−65 [−60]	34.4
optPBE-vdW	(AB) 3.40 [3.41]	−60 [−56]	—
	(AA′) 3.41 [3.42]	−60 [−56]	28.1
vdW-DF2	(AB) 3.51 [3.54]	−47 [−43]	—
	(AA′) 3.49 [3.55]	−47 [−43]	28.3
DFT-D2	(AB) 3.07 [3.10]	−79 [−74]	—
	(AA′) 3.08 [3.11]	−77 [−71]	55.0
LDA	(AB) 3.21 [3.29]	−28 [−24]	32.4
PBE	∼4	∼ −2	—
Other work			
LDA	(AA′) 3.24 [63]	—	—
	(AB) 3.24 [64]	—	—
	(AA′) 3.25 [64]	—	—
vdW-DF for layered materials	3.63 [15]	−26 [15]	—
vdW-DF	3.54 [46]	−51 [46]	—
vdW-DF2	3.44 [46]	−51 [46]	—
TS-PBE	(AA′) 3.33 [47]	−86 [47]	—
RPA+	3.31 [66]	—	—
Experiment	(AA′) 3.33 [67]	—	32.4 [68]

interlayer spacing by ∼6% (3.54 Å) in our calculations. The optB88-vdW functional gives both an interlayer distance and binding energy in reasonable agreement with experiment: 3.36 Å and −65 meV/atom, respectively. Still better agreement is obtained with optPBE-vdW for the binding energy (−60 meV/atom), but in this case the interlayer distance is overestimated by ∼5% (3.46 Å). In previous vdW-DF calculations, using either the original Dion *et al* version of vdW-DF or vdW-DF2, good values for the interlayer energy were obtained but the interlayer distances were overestimated by about 0.2 Å [45] and 0.1 Å [46, 62], respectively, and in line with our results obtained with vdW-DF2. Hence, we found here that the optB88-vdW and optPBE-vdW functionals offer a slight improvement over previous vdW-DF calculations. Likewise for this system, the new vdW functionals outperform the Tkatchenko–Scheffler (TS) correction scheme, which although often very accurate, predicts a large interlayer binding energy of −85 meV/atom. In addition, the elastic constant in the *c*-direction, C_{33}, has been calculated for each functional (except for PBE for which essentially no binding is obtained). The results in table 2 show that all functionals predict a value within ±4 GPa of experiment (36 ± 1 GPa) [60]. Particularly good is the performance of the DFT-D2 and optB88-vdW functionals which yield values of 36 and 38 GPa, respectively.

Let us now turn to h-BN and consider how the various functionals perform for B–N bond length and atomization energies, and then interlayer binding. Table 3 reveals that, as with graphite, all functionals give values for the B–N bond length (∼1.45 Å), in very good agreement with experiment [65]. From the computed atomization energies, LDA gives a slightly large value (−8.0 eV/atom) in line with previous LDA calculations [63] and vdW-DF2 slightly underestimates this energy. All other functionals give similar atomization energies of around −7.0 eV/atom.

Concerning interlayer distances, the experimental value is the same as graphite, 3.33 Å [67]. For the interlayer binding energy, experimental values are not available; however, some preliminary considerations can still be made. The results for h-BN interlayer distances and interlayer binding energies

calculated with the functionals considered in this study are reported in table 4 and figure 2. The results show that, as with graphite, PBE does not reproduce any binding between layers, except for a negligible minimum (~ -2 meV/atom) at around 4 Å. LDA gives better results than PBE since it predicts a clear interlayer binding minimum of -28 meV/atom at 3.1 Å. vdW-DF2 predicts an interlayer binding energy in the same range as for graphite but, as in the case of graphite, overestimates the interlayer spacing by ∼5%. The optPBE-vdW and optB88-vdW functionals reproduce interlayer distances in good agreement with experiment, ∼3.3–3.4 Å, and the calculated interlayer binding energies obtained are around 60–65 meV/atom. Quite large values for the binding energy are also obtained in our DFT-D2 calculations, ~ -80 meV/atom, and a rather poor interlayer separation of 3.08 Å is obtained. Indeed the interlayer binding energy predicted by DFT-D2 is almost 20 meV larger than it is for graphite. This is inconsistent with the other approaches (all the vdW-DFs and PBE-TS) and due to the particular choice of C_6 coefficients used in the DFT-D2 scheme, as discussed in section 4. Our computed binding energies cannot at this point be compared to experiment but they can, of course, be compared to previous theoretical work with vdW-corrected DFT approaches. This reveals that the values obtained sit roughly in the middle of a broad range which extends from -26 to -86 meV/atom. The -26 meV/atom value comes from the vdW-DF for layered materials introduced in [15]. This appears to be an unrealistically low value for the binding energy since it is similar to LDA and also associated with a large interlayer spacing of 3.6 Å. The vdW-DF and vdW-DF2 functionals also predict rather large interlayer spacings of 3.54 and 3.44 Å, respectively, with interlayer binding energies both of -51 meV/atom, in line with our calculations performed with the vdW-DF2 functional. At the upper end of the range is the PBE-TS scheme. It seems likely that, as was the case with graphite, this functional slightly overestimates the interlayer binding energy. However, the interlayer spacing predicted by PBE-TS coincides exactly with the experimental value.

Also for h-BN, the C_{33} constant has been evaluated (table 4). In this case the spread of results for each functional is larger than we saw for graphite. LDA performs particularly well, predicting a value in very good agreement with experiments. The DFT-D2 functional, that performed very well for graphite, predicts a C_{33} (55.0 GPa) ∼70% larger than experiment (32.4 GPa) [68]. The optPBE-vdW and the vdW-DF2 functionals predict values about 4 GPa smaller than experiment while optB88-vdW predicts a value 2 GPa larger.

4. Discussion and conclusions

It is interesting at this stage to compare the values obtained for the interlayer binding energy of graphite and h-BN. Looking at the results from all the functionals considered in this study and in previous work, almost all predict that the interlayer binding energy of graphite and h-BN is the same to within a few meV. The exception is the DFT-D2 approach which, because of the larger average C_6 coefficient of boron and nitrogen compared to carbon[7], predicts an interlayer binding energy ∼30% larger for h-BN compared to graphite. The interlayer separation predicted by DFT-D2 for h-BN is also considerably shorter than the values obtained from the other functionals and so it looks likely that DFT-D2 is overestimating the interlayer h-BN interaction. Since all the other approaches predict such similar interlayer binding energies, it is interesting to consider why this is the case. To this end we decomposed the various contributions to the interlayer binding energies obtained from optB88-vdW. Specifically we decomposed the interlayer binding energy, $E_{\mathrm{inter(tot)}}$, into:

$$E_{\mathrm{inter(tot)}} = E_{\mathrm{local(c)}} + E_{\mathrm{nl(c)}} + E_{\mathrm{rest}}, \tag{5}$$

where $E_{\mathrm{local(c)}}$ is the local correlation contribution to the total interlayer binding energy, $E_{\mathrm{nl(c)}}$ is the non-local correlation energy to the binding energy and E_{rest} is the remaining contribution to the binding energy coming from all other components of the Kohn–Sham energy. The results obtained from this decomposition for the optB88-vdW functional at an interlayer separation of 3.3 Å are reported in figure 3. The first thing to note from figure 3 is that all the components of the total energy are very similar and that there are no dramatic differences between the two materials in terms of

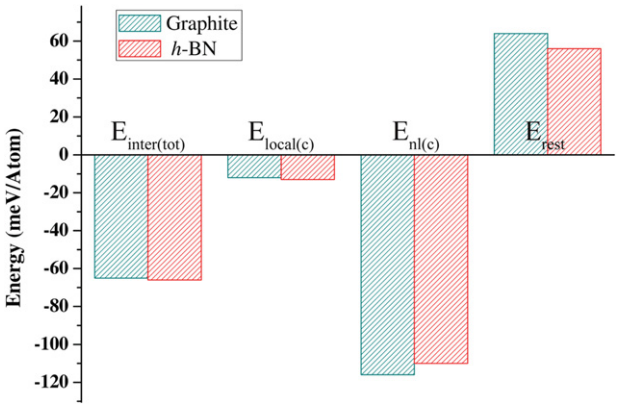

Figure 3. Decomposition of the interlayer binding energies of graphite and h-BN obtained with the optB88-vdW functional for an interlayer distance of 3.3 Å. The columns on the left are the total interlayer binding energies ($E_{\mathrm{inter(tot)}}$), which are decomposed into local correlation ($E_{\mathrm{local(c)}}$), non-local correlation ($E_{\mathrm{nl(c)}}$) and the remaining Kohn–Sham energy (E_{rest}) respectively.

[7] The relevant C_6 coefficients in DFT-D2 are: $C_6^{\mathrm{B}} = 3.13$, $C_6^{\mathrm{C}} = 1.75$, $C_6^{\mathrm{N}} = 1.23$ (see [51]). This leads to a C_6^{BN} coefficient ∼10% larger than C_6^{CC}, which agrees very well with the observed 9 meV difference between interlayer binding energies of graphite and h-BN. In contrast, the optB88-vdW and optPBE-vdW functionals reproduce almost the same interlayer binding energy for both materials. We therefore compared the non-local corrections for graphite and h-BN obtained with the optB88-vdW functional with the D2 corrections for both materials. The non-local corrections for graphite and h-BN are $E_{\mathrm{c}}^{\mathrm{nl}}(\mathrm{G}) = 116$ meV and $E_{\mathrm{c}}^{\mathrm{nl}}(\mathrm{BN}) = 110$ meV, respectively. In order to compare these values with the D2 corrections, DFT-D2 calculations with the LDA correlation energy have been performed since the non-local correction contains some PBE-like semilocal correlation (see equation (1)). We observed also in this case that the D2-correction for h-BN is ∼9 meV larger than that for graphite, while the van der Waals scheme produced non-local corrections ∼6 meV smaller.

the overall bonding decomposition. Looking more closely, however, we see that the local correlation energy contribution is almost the same for both graphite and h-BN (∼1 meV larger for h-BN) while the non-local correlation energy is ∼6 meV more negative (i.e., more attractive) for graphite than for h-BN. On the other hand, the rest of the energy where the exchange and the electrostatic contributions are included is ∼8 meV larger for graphite (i.e., more repulsive). Although all these energy differences are small, it is clear therefore that graphite and h-BN have similar interlayer binding energy because the stronger electrostatic interaction of h-BN (due to the polarity of the material) is compensated for by the stronger dispersive interaction in graphite. This analysis is consistent with the excellent recent studies reported by Hod [74] and Björkman *et al* [5], which found similarities in interlayer binding energies for a large class of layered materials. In agreement with our analysis, this was attributed to a balance between repulsion and attractive interactions.

Finally, to conclude, we have presented results from a range of exchange–correlation functionals for the binding in graphite and h-BN. This has included results from the new optB88-vdW and optPBE-vdW functionals and a comparison with previous dispersion-corrected DFT studies on graphite and h-BN. Overall we conclude that the optB88-vdW and optPBE-vdW functionals provide a fairly computationally inexpensive means (e.g., compared to PBE, the calculation of bulk graphite takes ∼24% more time) of obtaining reasonably accurate interlayer and intralayer structural and energetic properties for both graphite and h-BN. These functionals offer better performance than the original vdW-DF of Dion *et al* for graphite and h-BN. An improved agreement with experimental values has been obtained especially in the description of structural parameters, intralayer bond lengths and interlayer spacings. Recent studies have found that these improvements also apply to graphene interacting with metal surfaces and for bulk metals [3, 69, 70]. This, along with previous work with the optB88-vdW and optPBE-vdW functionals [3, 6, 27–31], suggests that a much broader range of systems can now be tackled with confidence with these functionals. There is, of course, much scope for improvement with regard to dispersion-corrected DFT studies of metals and semi-metals, in particular in understanding the role of many-body correlation [71–73]. Despite the obvious differences, we see here that graphite and h-BN have similar interlayer spacings and interlayer binding energies. Our analysis of the various contributions to the interlayer binding energy reveals that this results from a cancelation of two terms. The polar nature of the h-BN means that the electrostatic contribution to the binding energy is more favorable than in graphite, an effect which is compensated for by the slightly greater dispersive contribution to interlayer binding in graphite. It will be interesting to see if a similar compensation of electrostatic and dispersion applies to the absorption of small molecules within graphite and h-BN. Work in this area, which may be relevant to hydrogen storage, is currently ongoing.

Acknowledgments

The UK Science and Technology Facilities Council is gratefully acknowledged for financial support in the form of a NEXT-DTC studentship for GG under Contract No. 4070006444. JK is grateful to UCL and EPSRC for support through the PhD+ scheme. FF-A thanks the Science and Technology Facilities Council for financial support. AM's work is supported by the European Research Council and Royal Society though a Royal Society Wolfson Research Merit Award. We are grateful to the London Centre for Nanotechnology, UCL Research Computing, and the STFC's e-Science facility for the computational resources.

References

[1] Antony J and Grimme S 2006 *Phys. Chem. Chem. Phys.* **8** 5287
[2] Cooper V R, Thonhauser T, Puzder A, Schröder E, Lundqvist B I and Langreth D C 2008 *J. Am. Chem. Soc.* **130** 1304
[3] Klimeš J, Bowler D R and Michaelides A 2011 *Phys. Rev.* B **83** 195131
[4] Tao J, Perdew J P and Ruzsinszky A 2010 *Phys. Rev.* B **81** 233102
[5] Björkman T, Gulans A, Krasheninnikov A V and Nieminen R M 2012 *Phys. Rev. Lett.* **108** 235502
[6] Carrasco J, Santra B, Klimeš J and Michaelides A 2011 *Phys. Rev. Lett.* **106** 026101
[7] Johnston K, Kleis J, Lundqvist B I and Nieminen R M 2008 *Phys. Rev.* B **77** 121404
[8] Chakarova-Käck S D, Schröder E, Lundqvist B I and Langreth D C 2006 *Phys. Rev. Lett.* **96** 146107
[9] Whitesides G M and Grzybowski B 2002 *Science* **295** 2418
[10] Hohenberg P and Kohn W 1964 *Phys. Rev.* **136** B864
[11] Kohn W and Sham L 1965 *Phys. Rev.* **140** A1133
[12] Dobson J F and Dinte B P 1996 *Phys. Rev. Lett.* **76** 1780
[13] Andersson Y, Langreth D C and Lundqvist B I 1996 *Phys. Rev. Lett.* **76** 102
[14] Hult E, Andersson Y, Lundqvist B I and Langreth D C 1996 *Phys. Rev. Lett.* **77** 2029
[15] Rydberg H, Dion M, Jacobson N, Schröder E, Hyldgaard P, Simak S I, Langreth D C and Lundqvist B I 2003 *Phys. Rev. Lett.* **91** 126402
[16] Dion M, Rydberg H, Schröder E, Langreth D C and Lundqvist B I 2004 *Phys. Rev. Lett.* **92** 246401
[17] Antony J, Ehrlich S, Grimme S and Krieg H 2010 *J. Chem. Phys.* **132** 154104
[18] Tkatchenko A and Scheffler M 2009 *Phys. Rev. Lett.* **102** 073005
[19] Harl J and Kresse G 2009 *Phys. Rev. Lett.* **103** 056401
[20] Becke A D and Johnson E R 2005 *J. Chem. Phys.* **122** 154104
[21] Adamson R D, Dombroski J P and Gill P M W 1999 *J. Comput. Chem.* **20** 921
[22] Lee K, Murray E D, Kong L, Lundqvist B I and Langreth D C 2010 *Phys. Rev.* B **82** 081101
[23] Perdew J P and Yue W 1986 *Phys. Rev.* B **33** 8800
[24] Murray E D, Lee K and Langeth D C 2009 *J. Chem. Theory Comput.* **5** 2754
[25] Becke A D 1988 *Phys. Rev.* A **38** 3098
[26] Perdew J P, Burke K and Ernzerhof M 1996 *Phys. Rev. Lett.* **77** 3865
[27] Klimeš J, Bowler D R and Michaelides A 2010 *J. Phys.: Condens. Matter* **22** 022201
[28] Hu X L, Carrasco J, Klimeš J and Michaelides A 2011 *Phys. Chem. Chem. Phys.* **13** 12447

[29] Lew W, Crowe M C, Campbell C T, Carrasco J and Michaelides A 2011 *J. Phys. Chem.* C **115** 23008
[30] Zhang C, Wu J, Galli G and Gygi F 2011 *J. Chem. Theory Comput.* **7** 3054
[31] Addato M A F, Rubert A A, Benítez G A, Fonticelli M H, Carrasco J, Carro P and Salvarezza R C 2011 *J. Phys. Chem.* C **115** 17788
[32] Bollmann W and Spreadborough J 1960 *Nature* **186** 29
[33] Enoki T, Endo M and Suzuki M 2003 *Graphite Intercalation Compounds and Applications* (Oxford: Oxford University Press)
[34] Wang L and Yang R T 2010 *Catal. Rev. Sci. Eng.* **52** 411
[35] Jhi S-H and Kwon Y-K 2004 *Phys. Rev.* B **69** 245407
[36] Lovell A, Fernandez-Alonso F, Skipper N T, Refson K, Bennington S M and Parker S F 2008 *Phys. Rev. Lett.* **101** 126101
[37] Pellenq R J, Marinelli F, Fuhr J D, Fernandez-Alonso F and Refson K 2008 *J. Chem. Phys.* **129** 224701
[38] Rairkar A, Adams J B and Ooi N 2005 *Carbon* **44** 231
[39] Girifalco L A and Hodak M 2002 *Phys. Rev.* B **65** 125404
[40] Kristyán S and Pulay P 1994 *Chem. Phys. Lett.* **229** 175
[41] Pérez-Jordá J and Becke A D 1995 *Chem. Phys. Lett.* **233** 134
[42] Spanu L, Sorella S and Galli G 2009 *Phys. Rev. Lett.* **103** 196401
[43] Kohn W, Meir Y and Makarov D E 1998 *Phys. Rev. Lett.* **80** 4153
[44] Grimme S 2004 *J. Comput. Chem.* **25** 1463
[45] Ziambaras E, Kleis J, Schröder E and Hyldgaard P 2007 *Phys. Rev.* B **76** 155425
[46] Hamada I and Otani M 2010 *Phys. Rev.* B **82** 153412
[47] Marom N, Bernstein J, Garel J, Tkatchenko A, Joselevich E, Kronik L and Hod O 2010 *Phys. Rev. Lett.* **105** 046801
[48] Hanke F 2011 *J. Comput. Chem.* **32** 1424
[49] Nozières P and Pines D 1958 *Phys. Rev.* **111** 442
[50] Lebègue S, Harl J, Gould T, Ángyán J G, Kresse G and Dobson J F 2010 *Phys. Rev. Lett.* **105** 196401
[51] Grimme S 2006 *J. Comput. Chem.* **27** 1787
[52] Kresse G and Hafner J 1993 *Phys. Rev.* B **47** 558
[53] Kresse G and Furthmüller J 1996 *Comput. Mater. Sci.* **6** 15
[54] Kresse G and Furthmüller J 1996 *Phys. Rev.* B **54** 11169
[55] Román-Pérez G and Soler J M 2009 *Phys. Rev. Lett.* **103** 096102
[56] Blöchl P E 1994 *Phys. Rev.* B **50** 17953
[57] Zacharia R, Ulbricht H and Hertel T 2004 *Phys. Rev.* B **69** 155406
[58] Peluso A and Fliszá S 1988 *Can. J. Chem.* **66** 2631
[59] Lide D R (ed) 2008 *CRC Handbook of Chemistry and Physics* (Boca Raton, FL: CRC Press)
[60] Mounet N and Marzari N 2005 *Phys. Rev.* B **71** 205214
[61] Chakarova-Käck S D, Vojvodic A, Kleis J, Hyldgaard P and Schröder E 2010 *New J. Phys.* **12** 013017
[62] Berland K, Borck Ø and Hyldgaard P 2011 *Comput. Phys. Commun.* **182** 1800
[63] Kresse G, Kern G and Hafner J 1999 *Phys. Rev.* B **59** 8551
[64] Liu L, Feng Y P and Shen Z X 2003 *Phys. Rev.* B **68** 104102
[65] Kabalkina S and Vereshchagin L 1961 *Sov. Phys. Dokl.* **5** 1065
[66] Marini A, García-González P and Rubio A 2006 *Phys. Rev. Lett.* **96** 136404
[67] Solozhenko V L, Will G and Elf F 1995 *Solid State Commun.* **96** 1
[68] Green J F, Bolland T K and Bolland J W 1976 *J. Chem. Phys.* **64** 656
[69] Mittendorfer F, Garhofer A, Redinger J, Klimeš J, Harl J and Kresse G 2011 *Phys. Rev.* B **84** 201401
[70] Li X, Feng J, Wang E, Meng S, Klimeš J and Michaelides A 2012 *Phys. Rev.* B **85** 085425
[71] Klimeš J and Michaelides A 2012 submitted
[72] von Lilienfeld O A and Tkatchenko A 2010 *J. Chem. Phys.* **132** 234109
[73] Tkatchenko A, DiStasio R A Jr, Car R and Scheffler M 2012 *Phys. Rev. Lett.* **108** 236402
[74] Hod O 2012 *J. Chem. Theory Comput.* **8** 1360–9